Generating Correlated QPSK Waveforms By Exploiting Real Gaussian Random Variables

Seifallah Jardak
Signals and Systems Department
Ecole Polytechnique de Tunisie (EPT)-University of Carthage
La Marsa, Tunis, Tunisia
Email: seifallah.jardak@gmail.com

Sajid Ahmed and Mohamed-Slim Alouini
Electrical Engineering Program
King Abdullah University of Science and Technology
Thuwal, Makkah Province, Saudi Arabia
Email: {sajid.ahmed, slim.alouini}@kaust.edu.sa

***Abstract*—The design of waveforms with specified auto- and cross-correlation properties has a number of applications in multiple-input multiple-output (MIMO) radar, one of them is the desired transmit beampattern design. In this work, an algorithm is proposed to generate quadrature phase shift-keying (QPSK) waveforms with required cross-correlation properties using real Gaussian random-variables (RV's). This work can be considered as the extension of what was presented in [1] to generate BPSK waveforms. This work will be extended for the generation of correlated higher-order phase shift-keying (PSK) and quadrature amplitude modulation (QAM) modulation schemes that can better approximate the desired beampattern.**

***Keywords*-Colocated antennas; constant-envelope waveforms; Hermite polynomials; multiple-input multiple-output (MIMO) radar.**

I. Introduction

Recently the researchers have considered the application of multiple-input multiple-output (MIMO) techniques developed for wireless communication systems to the radar systems. In MIMO communication systems multiple antennas are deployed at the transmitter and receiver to increase the data rate and provide multiple paths to mitigate the fading in the channel. Like MIMO communications, MIMO radar offers a new paradigm for signal processing research. It possess significant potential for scintillation mitigation by illuminating the object from multiple transmit antennas as well as significant gain in detection through diversity gain and resolution enhancement through spatial resolution gain. In contrast to conventional phased-array radars, where all the waveforms are fully correlated, MIMO radars can transmit partially correlated waveforms that can provide extra degrees-of-freedom (DOF) [2], [3]. Signals transmitted by MIMO radar (also called probing signals) can be designed to approximate a desired transmit beampattern.

The design of desired beampattern using MIMO radar requires specified cross-correlation properties. The design of constant-envelope (CE) waveforms for given cross-correlation properties is challenging and it becomes more difficult when the requirement is to have finite-alphabet CE waveforms. For given cross-correlation properties, in [4], an iterative algorithm is used that generate infinite-alphabet CE waveforms, which are not typically desired in practice. The work in [1], proposes a new technique to generate finite alphabet CE waveforms for the given covariance matrix by mapping Gaussian random-variables (RV's) onto binary phase shift-keying (BPSK) symbols, using the $\mathrm{sign}(\cdot)$, function. In this technique the cross-correlation relationship between the Gaussian and BPSK RV's is developed, which make it easy to generate a BPSK waveform. The only drawback of this technique is that the sine inverse of the covariance matrix of Gaussian RV's corresponding to the given covariance matrix must be positive semidefinite.

In this paper, to approach the performance of infinite alphabet CE waveforms generated in [4], quadrature phase shift-keying (QPSK) waveforms are generated using real Gaussian RV's. In the proposed scheme, in contrast to [1], real Gaussian RV's are mapped on complex exponents to generate QPSK waveforms. In this paper, the cross-correlation relationship between the Gaussian and QPSK RV's is derived. In our on going research real and complex Gaussian RV's will be mapped to generate high order phase shift-keying (PSK) and quadrature amplitude modulation (QAM) waveforms. It is expected that as we increase the number of alphabets in the waveforms, the mean-squared-error (MSE) between the designed and the desired beampatterns will decrease.

The organization of the paper is as follows. In the following section the problem is formulated. In section III, the relationship between QPSK and real Gaussian RV's is derived. Simulation results are presented in Section IV. Finally, conclusion is drawn in Section V.

II. Problem Formulation

The problem is to maximize the transmitted power in the predefined region and minimize it in all other directions. This problem is also called beampattern matching and has applications in imaging. For this, consider a uniform linear

array of M antenna elements at the transmitter with half-wavelength inter-element spacing. If $x_m(n)$ is the baseband transmitted signal from antenna m at time index n and θ_k is the spatial location then the baseband received signal at location θ_k can be written as

$$r_k(n) = \sum_{m=1}^{M} e^{-j(m-1)\pi \sin(\theta_k)} x_m(n), \quad n = 1, 2, \ldots, N, \tag{1}$$

where N denotes the total number of symbols transmitted from one antenna. By defining $\mathbf{e}(\theta_k) = [1 \quad e^{j\pi \sin(\theta_k)} \quad \ldots \quad e^{j(M-1)\pi \sin(\theta_k)}]^T$ and $\mathbf{x}(n) = [x_1(n) \quad x_2(n) \quad \ldots \quad x_M(n)]^T$, the received signal in (1) can be written in vector form as

$$r_k(n) = \mathbf{e}^H(\theta)\mathbf{x}(n). \tag{2}$$

Following (2), the received power at location θ_k can be written as

$$\begin{aligned} P(\theta_k) &= E\left\{\mathbf{e}^H(\theta)\mathbf{x}(n)\mathbf{x}^H(n)\mathbf{e}(\theta)\right\} \\ &= \mathbf{e}^H(\theta)\mathbf{R}\mathbf{e}(\theta), \end{aligned} \tag{3}$$

where $\mathbf{R}$ is the correlation matrix of the transmitted waveforms. Let $\phi(\theta)$ denotes the desired transmit beampattern, we divide the region of interest into K equally spaced angular locations. In order to achieve the desired beampattern match, the following cost-function needs to be minimised with respect to the covariance vector $\mathbf{R}$,

$$J(\mathbf{R}) = \frac{1}{K}\sum_{k=1}^{K}\left(\mathbf{e}^H(\theta_k)\mathbf{R}\mathbf{e}(\theta_k) - \alpha\phi(\theta_k)\right)^2, \tag{4}$$

where α is a scaling factor. Since R is a covariance matrix and for maximum power efficiency, all the antennas are required to transmit at the same maximum power level (due to the non-linearity of transistors). Therefore, $\mathbf{R}$ must satisfy the following constraints

$$\begin{aligned} &\mathbf{C}_1. \qquad \mathbf{v}^H\mathbf{R}\mathbf{v} \geq 0, \qquad \text{for all } \mathbf{v} \\ &\mathbf{C}_2. \qquad \mathbf{R}(m,m) = c, \qquad \text{for } m = 1, 2, \ldots, M, \end{aligned} \tag{5}$$

where c is the transmitted power from the antenna m. Once $\mathbf{R}$ is synthesized, its corresponding waveform matrix $\mathbf{X} = \left[\begin{array}{cccc} \mathbf{x}_1 & \mathbf{x}_2 & \cdots & \mathbf{x}_M \end{array}\right]$ can be easily generated as

$$\mathbf{X} = \mathcal{X}\mathbf{\Lambda}^{1/2}\mathbf{W}^H, \tag{6}$$

where $\mathbf{X} \in \mathcal{C}^{N\times M}$, $\mathbf{x}_m$ contains the symbols to be transmitted from antenna m, $\mathcal{X}$ is a matrix of zero mean and unit variance Gaussian RV's, $\mathbf{\Lambda} \in \mathcal{R}^{M\times M}$ is the diagonal matrix of eigenvalues and $\mathbf{W} \in \mathcal{C}^{M\times M}$ is the matrix of eigenvectors of $\mathbf{R}$. As $\mathbf{X}$ is Gaussian, it can not guarantee a finite alphabet CE solution and may have high peak-to-average-power-ratio (PAPR).

In the next section, Gaussian RV's are mapped onto the memoryless complex exponential functions to generate QPSK RV's.

III. Generation of QPSK waveforms from real Gaussian RV's

Let $\mathbf{R}$ be the covariance matrix of the QPSK waveforms and $\mathbf{R}_g$ be the covariance matrix of Gaussian RV's. Following (6), generating the matrix of real Gaussian RV's $\mathbf{X} = \left[\begin{array}{cccc} \mathbf{x}_1 & \mathbf{x}_2 & \cdots & \mathbf{x}_M \end{array}\right]$ to realize the given covariance matrix $\mathbf{R}_g$ is straightforward.

If the QPSK RV's $y_p = f(x_p)$ and $y_q = f(x_q)$ are respectively the non-linear functions of real Gaussian RV's x_p and x_q, then the cross correlation between y_p and y_q, $\psi_{pq} = E\{y_p y_q^*\}$, can be defined as

$$\psi_{pq} \equiv \int_{-\infty}^{+\infty}\int_{-\infty}^{+\infty} y_p y_q^* p(x_p, x_q, \rho_{pq}) dx_p dx_q, \tag{7}$$

where $p(x_p, x_q, \rho_{pq}) \equiv \frac{1}{2\pi\sqrt{1-\rho_{pq}}} e^{-\frac{x_p^2 - 2\rho_{pq} + x_q^2}{2(1-\rho_{pq}^2)}}$ is the joint probability distribution function (PDF) of x_p and x_q, and $\rho_{pq} = \frac{E(x_p x_q)}{\sigma_p \sigma_q}$ is the cross correlation coefficient of x_p and x_q.

In the case x_p and x_q have the same variance, i.e., $\sigma_p = \sigma_q = \sigma$, using the Hermite polynomial [5], the cross-correlation relationship in (7) can be written as

$$\begin{aligned} \psi_{pq} = \sum_{n=0}^{+\infty} \frac{\rho_{pq}^n}{2^n n!} &\int_{-\infty}^{+\infty} f(x) H_n\left(\frac{x}{\sigma\sqrt{2}}\right) p(x) dx \\ &\times \int_{-\infty}^{+\infty} f^*(x) H_n\left(\frac{x}{\sigma\sqrt{2}}\right) p(x) dx, \end{aligned} \tag{8}$$

where $f(x)$ is the memoryless non-linear mapping function, $p(x)$ is the PDF of real Gaussian RV and $H_n(x)$ are the physicists' Hermite polynomials.

If the memoryless non-linear function $f(x)$ is defined as

$$f(x) = e^{j\frac{pi}{4}\left(2\text{sign}\left(\frac{x}{\sigma\sqrt{2}}\right) + \text{sign}\left(1 - \left(\frac{x}{\sigma\sqrt{2}}\right)^2\right)\right)}, \tag{9}$$

where x is real Gaussian RV, then $y = f(x)$ will generate QPSK waveform with covariance matrix $\mathbf{R}(p,q) = \psi_{pq}$ for $p, q = 1, 2, \ldots, M$. We can also define $f(x)$ as follows

$$f(x) = \frac{\sqrt{2}}{2}\left[\text{sign}\left(\left(\frac{x}{\sigma\sqrt{2}}\right)^3 - \frac{x}{\sigma\sqrt{2}}\right) + j\ \text{sign}\left(\frac{x}{\sigma\sqrt{2}}\right)\right]. \tag{10}$$

Because both mapping functions give the same result, we derived (8) using only the first definition of $f(x)$ as in (9).

By solving (8) the relationship between the correlation of Gaussian and QPSK RV's can be found as (please see the appendix for the proof)

$$\psi_{pq} = \frac{2}{\pi}\sum_{n=0}^{+\infty} \underbrace{\frac{\rho_{pq}^{2n+1}(|2n-1|)!!}{(2n+1)(2n)!!}}_{\text{First factor}} \underbrace{\left(1 + 2e^{-1}a_n + 2e^{-2}a_n^2\right)}_{\text{Second factor}}, \tag{11}$$

where

$$a_n = \begin{cases} a_0 & = (-1) \\ a_1 & = 1 \\ a_{n+2} & = 2a_{n+1} - a_n \\ & \quad -4\sum_{i=0}^{n} \frac{C_n^i (-2)^i}{(2i+3)!!} \quad \forall n \in \mathbb{N}. \end{cases} \tag{12}$$

Fig. 1 shows the cross-correlation relationship between the Gaussian and QPSK RV's. The first term in (11) corresponds to the Taylor series of the sine inverse function.

$$\sum_{n=0}^{+\infty} \frac{\rho_{pq}^{2n+1}(|2n-1|)!!}{(2n+1)(2n)!!} = \sin^{-1}(\rho_{pq}). \tag{13}$$

However, apart from the first three terms, the series a_n oscillates with an increasing period as shown in Fig. 2.

So far, we have not found a compact function for this relationship. Therefore, the infinite sum in (11) is approximated. To determine the approximation function, which is denoted by g, different types of functions were tested and the following approximation gave best result in terms of approximating the exact function

$$\begin{aligned} \psi_{pq} &= g(\rho_{pq}) \\ &= \frac{2}{\pi} \frac{\sin^{-1}(\rho_{pq})}{1.866 - 0.866\rho_{pq}^2}. \end{aligned} \tag{14}$$

Following the relationship in (14), we can write

$$\mathbf{R} = g(\mathbf{R}_g).$$

It can be easily proved that if $\mathbf{R}_g$ is positive semidefinite, then $\mathbf{R}$ will be positive semidefinite. To obtain positive semidefinite and equal diagonal matrix $\mathbf{R}_g$, the algorithm given in [1] is used. The elements of $\mathbf{R}$ are obtained using the particle-swarm-optimization (PSO) algorithm given in

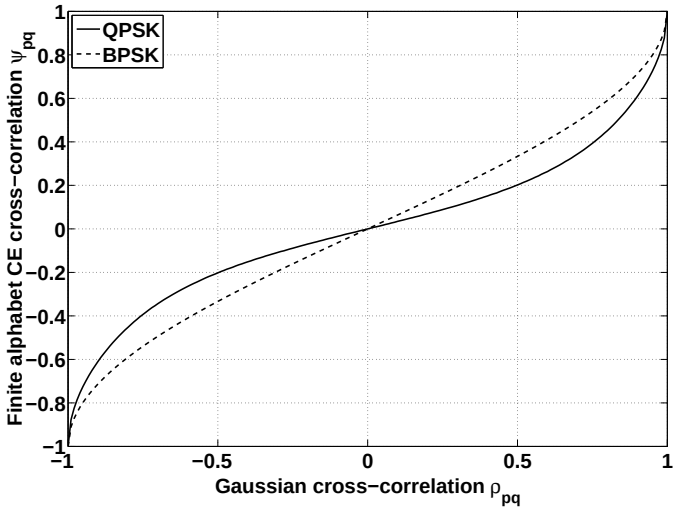

Fig. 1. The cross-correlation relationship between the mapped Gaussian and QPSK RV's.

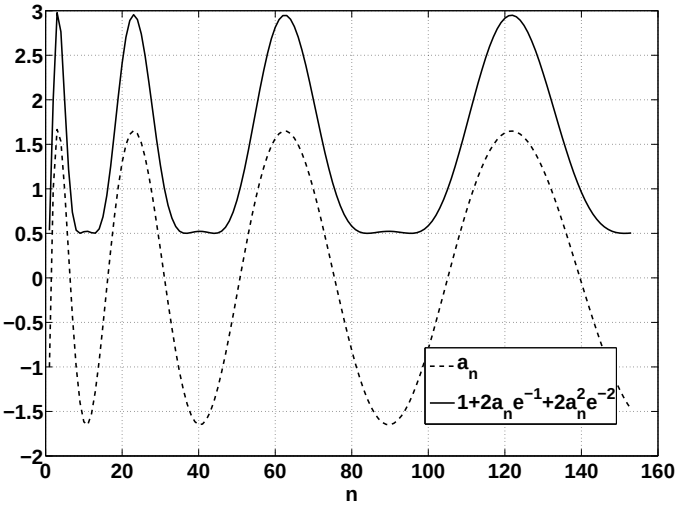

Fig. 2. The behaviour of the a_n coefficients as function of n.

[6] to minimize the following cost function

$$J(\mathbf{R}_g) = \frac{1}{K} \sum_{k=1}^{K} \left(\mathbf{e}^H(\theta_k) g(\mathbf{R}_g) \mathbf{e}(\theta_k) - \alpha\phi(\theta_k) \right)^2. \tag{15}$$

IV. Simulation Results

In this section, several examples are presented to validate the performance of the proposed algorithm. For all simulations, the number of transmit antennas is 10 and inter-element spacing is half of the wavelength.

In the first simulation, we want to transmit maximum power between -30 to $+30$ degrees. Fig. 3(a) shows the convergence behaviour of PSO to synthesise the covariance matrix $\mathbf{R}_g$ so to generate BPSK [1] and QPSK waveforms for the desired beampattern. It can be seen in the figure that although the PSO algorithm converges faster for BPSK waveforms, it converges to lower MSE for QPSK waveforms. The advantage of lower MSE can be seen in the Fig. 3(b), where the corresponding desired beampattern is compared with the beampattern designed using BPSK and QPSK waveforms. The designed beampattern using QPSK waveforms has lower side lobes and lower ripples in the maximum power region.

In the second simulation, the desired maximum power region is divided into two separate regions, the first one is between -45 to -15 degrees while the second one is between 15 to 45 degrees. Fig. 4(a) shows the convergence behaviour of PSO to synthesise the covariance matrix $\mathbf{R}_g$ so to generate BPSK [1] and QPSK waveforms for this beampattern. Here again, to generate BPSK waveforms, the PSO algorithm converges faster than to generate QPSK waveforms. For this simulation, it can be noted that the MSE of QPSK waveform is again lower than BPSK waveforms, however the MSE difference is smaller compared to

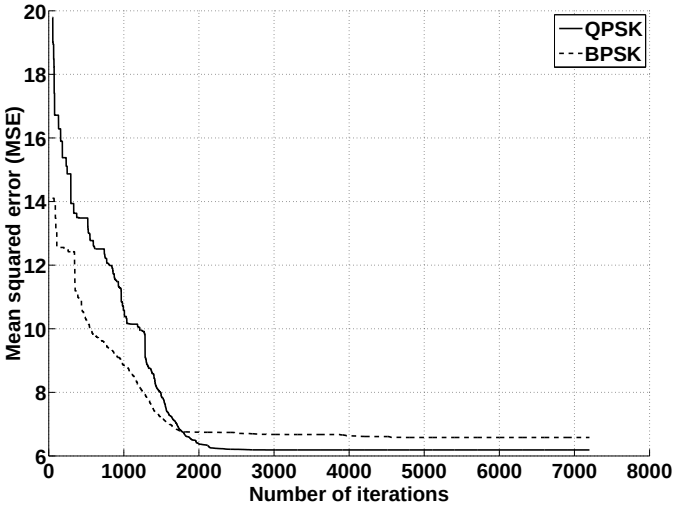

(a) Convergence performance

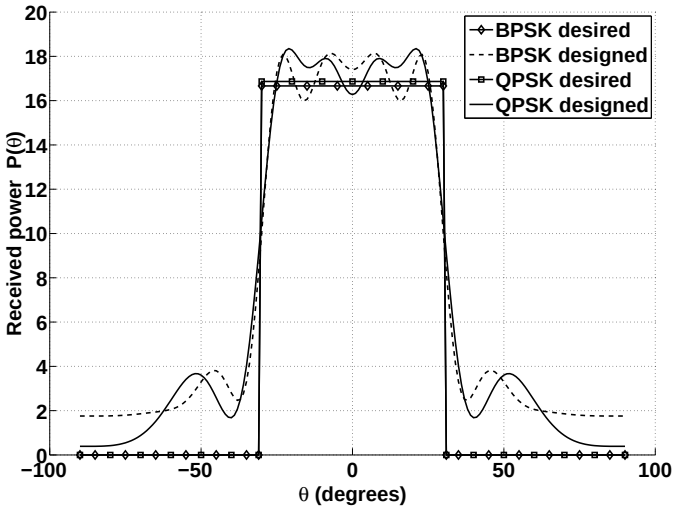

(b) Designed beampattern

Fig. 3. Convergence performance (a) and designed beampattern (b) in case the region of interest is $[-30^\circ, 30^\circ]$.

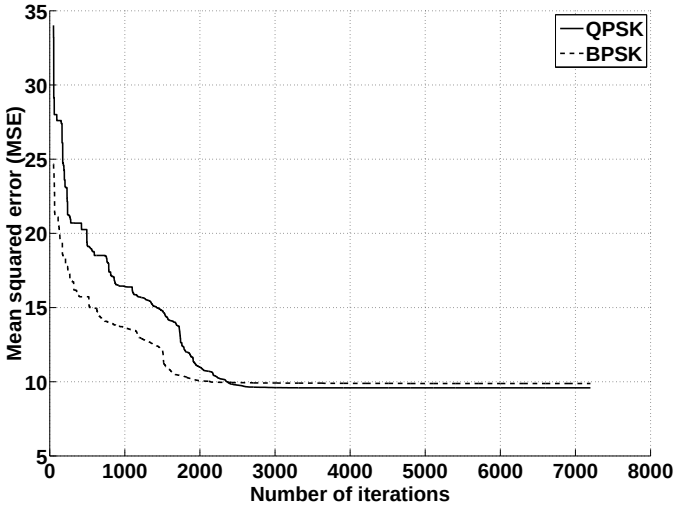

(a) Convergence performance

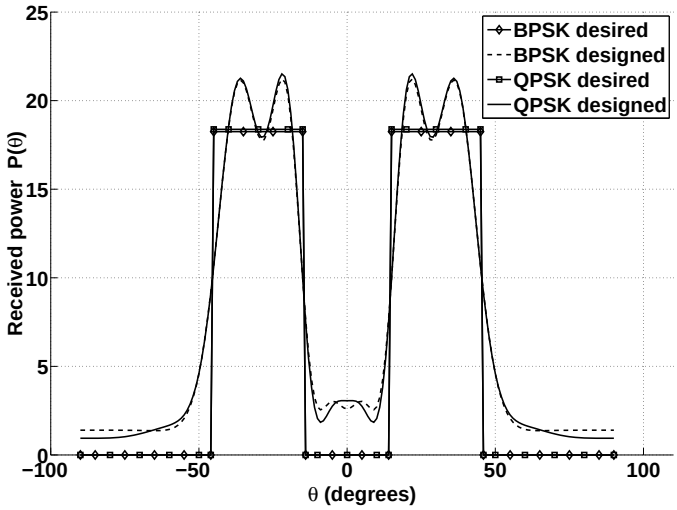

(b) Designed beampattern

Fig. 4. Convergence performance (a) and designed beampattern (b) in case the region of interest is $[-45^\circ, -15^\circ]$ and $[15^\circ, 45^\circ]$.

the previous simulation. Similarly, Fig. 4(b) compares the desired beampattern with the beampatterns obtained using corresponding BPSK and QPSK waveforms. Since in this simulation, the MSE difference is small, QPSK waveforms do not significantly outperform BPSK waveforms.

V. Conclusion

The goal of this paper was to present a finite alphabet CE waveform generation algorithm to obtain the desired beampatterns. The proposed algorithm maps real Gaussian RV's onto QPSK symbols and suggests an approximation to the cross-correlation relationship between the real Gaussian and the QPSK RV's. Since the inverse of the approximation function does not preserve the property of positive semidefinite of QPSK cross correlation matrix, we synthesized directly the covariance matrix of Gaussian RV's by means of the particle swarm optimization algorithm. At the end, we compared the performance of BPSK and QPSK waveforms and we showed that QPSK waveforms perform better.

Appendix

Consider real Gaussian RVs x_p and x_q mapped onto QPSK RVs y_p and y_q as follows

$$y_p = e^{j\frac{pi}{4}\left(2\text{sign}\left(\frac{x_p}{\sigma\sqrt{2}}\right)+\text{sign}\left(1-\left(\frac{x_p}{\sigma\sqrt{2}}\right)^2\right)\right)} = f\left(\frac{x_p}{\sigma\sqrt{2}}\right),$$
$$y_q = e^{j\frac{pi}{4}\left(2\text{sign}\left(\frac{x_q}{\sigma\sqrt{2}}\right)+\text{sign}\left(1-\left(\frac{x_q}{\sigma\sqrt{2}}\right)^2\right)\right)} = f\left(\frac{x_q}{\sigma\sqrt{2}}\right), \quad (16)$$

where σ is the variance of the Gaussian RVs. Using (8), we can write the relationship between the cross correlation of real Gaussian and QPSK RVs as follows:

$$\psi_{pq} = \sum_{n=0}^{+\infty} \frac{\rho_{pq}^n}{2^n n!} \times \int_{-\infty}^{+\infty} f\left(\frac{x}{\sigma\sqrt{2}}\right) H_n\left(\frac{x}{\sigma\sqrt{2}}\right) p(x)dx \times \int_{-\infty}^{+\infty} f^*\left(\frac{x}{\sigma\sqrt{2}}\right) H_n\left(\frac{x}{\sigma\sqrt{2}}\right) p\left(x\right) dx. \quad (17)$$

If we substitute $\tilde{x} = \frac{x}{\sigma\sqrt{2}}$ and we take into consideration the fact that f is an odd function, the above expression (17) can be reformulated as:

$$\psi_{pq} = \sum_{n=0}^{+\infty} \frac{\rho_{pq}^n}{2^n \pi n!} \times \int_0^{+\infty} f(\tilde{x})(H_n(\tilde{x}) - H_n(-\tilde{x}))e^{-\tilde{x}^2} d\tilde{x} \times \int_0^{+\infty} f(\tilde{x})(H_n(\tilde{x}) - H_n(-\tilde{x}))e^{-\tilde{x}^2} d\tilde{x}. \quad (18)$$

Besides, $H_n(-x) = (-1)^n H_n(x)$ [7] and given that f is constant between $[0, 1]$ and $[1, +\infty]$, we can write

$$\psi_{pq} = \sum_{n=0}^{+\infty} \frac{2\rho_{pq}^{2n+1}}{2^{2n}\pi(2n+1)!} \left[\left(\int_0^1 H_{2n+1}(\tilde{x}) e^{-\tilde{x}^2} d\tilde{x} \right)^2 + \left(\int_1^{+\infty} H_{2n+1}(\tilde{x}) e^{-\tilde{x}^2} d\tilde{x} \right)^2 \right]. \quad (19)$$

Reference [7] gives the expressions of the integrals used in (19)

$$\begin{aligned} A_n &= \int_0^1 H_{2n+1}(\tilde{x}) e^{-\tilde{x}^2} d\tilde{x} \\ &= (-1)^n \quad \frac{(2n+1)!}{n!} \quad {}_2F_2\left(\frac{2n+3}{2}, 1, \frac{3}{2}, 2, (-1)\right) \\ &= \underbrace{(-1)^n \frac{2n!}{n!}}_{B_n} \quad \underbrace{\sum_{k=0}^{+\infty} (-1)^k \frac{(2n+2k+1)!n!}{(n+k)!(2k+1)!(k+1)(2n)!}}_{C_n}. \end{aligned}$$

$$\begin{aligned} D_n &= \int_1^{\infty} H_{2n+1}(\tilde{x}) e^{-\tilde{x}^2} d\tilde{x} \\ &= \int_0^{\infty} H_{2n+1}(\tilde{x}) e^{-\tilde{x}^2} d\tilde{x} - \int_0^1 H_{2n+1}(\tilde{x}) e^{-\tilde{x}^2} d\tilde{x} \\ &= \underbrace{(-1)^n \frac{2n!}{n!}}_{B_n} - \underbrace{\int_0^1 H_{2n+1}(\tilde{x}) e^{-\tilde{x}^2} d\tilde{x}}_{A_n} \\ &= B_n - A_n = B_n - B_n C_n = B_n(1 - C_n). \end{aligned}$$

Therefore, (19) can be further simplified to

$$\psi_{pq} = \sum_{n=0}^{+\infty} \frac{2\rho_{pq}^{2n+1}}{2^{2n}\pi(2n+1)!} B_n^2 \left(1 - 2C_n + 2C_n^2\right), \quad (20)$$

where

$$C_n = (2n+1) \quad {}_2F_2\left(\frac{2n+3}{2}, 1, \frac{3}{2}, 2, (-1)\right),$$

and

$$B_n = (-1)^n \frac{2n!}{n!}.$$

However, C_n can be expressed differently as shown below

$$C_n \quad = 1 + a_n e^{-1} \quad (21)$$

$$\text{where} \quad a_n = \begin{cases} a_0 & = (-1) \\ a_1 & = 1 \\ a_{n+2} & = 2a_{n+1} - a_n \\ & \quad -4\sum_{i=0}^{n} \frac{C_n^i (-2)^i}{(2i+3)!!} \quad \forall n \in \mathbb{N}. \end{cases} \quad (22)$$

Using (21), the relationship between ψ_{pq} and ρ_{pq} can be finally written as follows

$$\psi_{pq} = \frac{2}{\pi} \sum_{n=0}^{+\infty} \frac{\rho_{pq}^{2n+1}(|2n-1|)!!}{(2n+1)(2n)!!} \left(1 + 2e^{-1}a_n + 2e^{-2}a_n^2\right). \quad (23)$$

REFERENCES

[1] S. Ahmed, J. Thompson, Y. Petillot, and B. Mulgrew, "Finite alphabet constant-envelope waveform design for mimo radar," *IEEE Transactions on Signal Processing*, vol. 59, no. 11, pp. 5326 –5337, Nov. 2011.

[2] E. Fishler, A. Haimovich, R. Blum, D. Chizhik, L. Cimini, and R. Valenzuela, "Mimo radar: an idea whose time has come," in *Proceedings of the IEEE Radar Conference*, Apr. 2004, pp. 71 – 78.

[3] E. Fishler, A. Haimovich, R. Blum, J. Cimini, L.J., D. Chizhik, and R. Valenzuela, "Spatial diversity in radars-models and detection performance," *IEEE Transactions on Signal Processing*, vol. 54, no. 3, pp. 823 – 838, Mar. 2006.

[4] P. Stoica, J. Li, and X. Zhu, "Waveform synthesis for diversity-based transmit beampattern design," *IEEE Transactions on Signal Processing*, vol. 56, no. 6, pp. 2593 –2598, Jun. 2008.

[5] J. Brown, J., "On the expansion of the bivariate gaussian probability density using results of nonlinear theory," *IEEE Transactions on Information Theory*, vol. 14, no. 1, pp. 158 – 159, Jan. 1968.

[6] J. Robinson and Y. Rahmat-Samii, "Particle swarm optimization in electromagnetics," *IEEE Transactions on Antennas and Propagation*, vol. 52, no. 2, pp. 397 – 407, Feb. 2004.

[7] A. Prudnikov, I. Brychkov, and O. Marichev, *Integrals and Series: Special functions*. Gordon and Breach Science Publishers, 1986.